Author Manuscript

Author Manuscript

Author Manuscript

Author Manuscript

HHS Public Access

Author manuscript

J Immunol. Author manuscript; available in PMC 2017 November 01.

Published in final edited form as:

J Immunol. 2016 November 1; 197(9): 3639–3649. doi:10.4049/jimmunol.1600402.

HIF-2α in Resting Macrophages Tempers Mitochondrial ROS to Selectively Repress MARCO-dependent Phagocytosis

Shirley Dehn[1,2], **Matthew DeBerge**[1,2], **Xin-Yi Yeap**[1,2], **Laurent Yvan-Charvet**[4], **Deyu Fang**[1], **Holger K. Eltzschig**[5], **Stephen D. Miller**[3], and **Edward B. Thorp**[1,2,*]

[1]Department of Pathology, Feinberg School of Medicine, Northwestern University, Chicago, IL

[2]Feinberg Cardiovascular Research Institute, Feinberg School of Medicine, Northwestern University, Chicago, IL

[3]Department of Microbiology & Immunology, Feinberg School of Medicine, Northwestern University, Chicago, IL

[4]Institut National de la Sante et de la Recherche Medicale (INSERM) U1065, Centre Mediterraneen de Medecine Moleculaire (C3M), Atip-Avenir, 06204 Nice, France

[5]University of Colorado Department of Anesthesiology

Abstract

Hypoxia Inducible Factor α (HIF-α) isoforms regulate key macrophage (Mϕ) functions during ischemic inflammation. HIF-2α drives pro-inflammatory cytokine production; however potential requirements for HIF-2α during other key Mϕ functions, including phagocytosis, are unknown. In contrast to HIF-1α, HIF-2α was not required for hypoxic phagocytic uptake. Surprisingly, basal HIF-2α levels under non-hypoxic conditions were both necessary and sufficient to suppress phagocytosis. Screening approaches revealed selective induction of scavenger receptor MARCO, which was required for enhanced engulfment. Chromatin IP identified the antioxidant NRF2 as directly responsible for inducing *Marco*. Concordantly, *Hif-2α*$^{-/-}$ Mϕs exhibited reduced antioxidant gene expression, and inhibition of mitochondrial reactive oxygen species (mROS) suppressed both *Marco* expression, and phagocytic uptake. *Ex vivo* findings were recapitulated *in vivo,* wherein the enhanced engulfment phenotype resulted in elevated bacterial clearance and cytokine suppression. Importantly, natural induction of *Hif-2α* by IL-4, also suppressed MARCO-dependent phagocytosis. Thus, unlike most characterized pro-phagocytic regulators, HIF-2α can act as a phagocytic repressor. This interestingly occurs in resting Mϕs through tempering of steady state mROS. In turn, HIF-2α promotes Mϕ quiescence by blocking a MARCO bacterial response pathway. IL-4 also drives HIF-2α suppression of MARCO, leading to compromised bacterial immuno-surveillance *in vivo.*

Keywords

phagocytosis; HIF-2α; MARCO; normoxic

*Correspondence: Department of Pathology, Feinberg School of Medicine, 390 East Superior St, Northwestern University, Chicago, IL 60611, USA.

Author Manuscript Author Manuscript Author Manuscript Author Manuscript

Introduction

Macrophages (Mϕs) are critical protagonists of phagocytosis, wound repair, and inflammation resolution, as they are mobilized at, and recruited to, sites of infection and tissue injury (1, 2). A common component of both infection and injury is reduction of intracellular oxygen tension (3–5). As reviewed extensively (6), decreases in molecular oxygen reduce the activity of oxygen-dependent prolyl hydroxylases (PHDs), thereby allowing Hypoxia Inducible Factors (7), master regulators of oxygen-regulated glycolysis, erythropoiesis, and angiogenesis, to escape VHL-mediated ubiquitination (8), proteosomal degradation, and in turn pair with HIF-1β (aryl hydrocarbon receptor nuclear translocator, or ARNT) (9). Hetero-dimerization of alpha and beta isoforms promote transcription (through pairing with transcriptional co-activators p300 and CBP) of genes encoding hypoxic response elements (HREs) (10).

In addition to sensitivities to molecular oxygen, alternative or non-hypoxic inflammatory triggers can activate HIFs, also independent of angiogenic signaling. For example, although hypoxia *per se* can suppress TLR expression (11), TLR stimulation by endotoxin can induce Mϕ HIF (12). Often this occurs with concomitant transcriptional reduction of prolyl hydoxylases (13). Also, key pro-inflammatory networks such as NF-kB (14) can activate HIFs (15) and vice versa (16).

HIF isoforms in Mϕs are differentially regulated by inflammatory ligands (12). Of the two primary isoforms, HIF-1α tissue expression is more selective, however, both are expressed in Mϕs wherein they encode overlapping and divergent functions. *Hif-1α* in Mϕs is required for glycolytic ATP production, which is critical in metabolically active inflammatory tissue, as well as bactericidal activity (17). As reported previously, HIF-1α in myeloid cells is critical for myeloid infiltration and activation (18).

HIF-2α in Mϕs interestingly can function independently of metabolic/ATP regulation: Previous studies indicate that Mϕ HIF-2α facilitates pro-inflammatory chemokine/cytokine production, independent of changes in cellular energy homeostasis, in contrast to Mϕ HIF-1α (19). *In vivo*, these studies also indicate that loss of myeloid *Hif-2α* protects from lipopolysaccharide-induced myocardial endotoxemia, in association with reduced chemokine and cytokine expression and leading to inhibited cellular migration and inflammation.

Phagocytic clearance by Mϕs is critical to wound repair and often occurs under limiting oxygen (20). Hypoxic induction of efferocytosis (the phagocytic uptake of apoptotic cells) has been linked to HIF-1α, through Mϕ scavenger receptor CD36 (21, 22). *However, the role in HIF-2α in efferocytosis, and other phagocytic pathways in general, is unknown*. Given our interest in tissue injury during hypoxia (20), the unique functions of HIF isoforms, and the importance of HIF-2α in inflammation, we first inquired into the role of HIF-2α during efferocytosis. We discovered a role for HIF-2α during phagocytic regulation, however surprisingly, HIF-2α acted in resting Mϕs, and also as a general phagocytosis suppressor. This HIF-2α mechanism of action is through suppression of mitochondrial ROS-dependent activation of the engulfment scavenger receptor, MARCO. As described herein,

Author Manuscript Author Manuscript Author Manuscript Author Manuscript

further *in vivo* studies revealed the mechanism to be pronounced during bacterial phagocytic uptake, also raising important implications between HIF-2α levels and susceptibility to infection.

Materials & Methods

Mice

Experiments were performed with 8- to 14-week old mice. Mice were housed and bred in a pathogen-free environment in the Vivarium of Northwestern University, Chicago, IL, and under IACUC approval. C57BL/6 mice (H-2^b) were used as WT mice unless otherwise designated. Mice with myeloid lineage-specific knockout of *Hif-1α* (*Hif-1α flox/flox, LysMCre and MxCre*) have previously been described (18). *Hif-2α* have also been described (23). LysMcre *LSL Hif-2α*$^{fl/fl}$ mice were generously from Yatrik Shah (24) and as previously described (25). *Hif-1β/Arnt−/−* mice were generously provided by F. Gonzalez (26). *Marco−/−* mice were from *S. Miller* at Northwestern University (27).

In vivo apoptotic cell and S. Aureus phagocytosis assays

Hif-2α$^{fl/fl}$ and *LysMcre,Hif-2α*$^{fl/fl}$ mice were injected with fluorescently labelled apoptotic Jurkats. Cells were stained with F4/80-PE and *in vivo* efferocytosis was quantified as percent of FITC-positive, F4/80 positive cells. For *Staphylococcus Aureus*: 200μL PBS containing 0.1% BSA with and without 100ng IL-4 at 0 and 16 hours. At 18 hours, mice were injected with 1x10^8 FITC-labeled *S. Aureus* bacteria in 200μL PBS with 0.1% BSA. 1 hour later, peritoneal infiltrate was harvested via PBS lavage.

Isolation of Splenic Mϕs

Spleens were harvested from *Hif-2α*$^{fl/fl}$ and *LysMcre,Hif-2α*$^{fl/fl}$ mice and filtered through a 70μm mesh strainer. Red blood cells were lysed and splenocytes stained for FACS analysis. Red Pulp Mϕs were gated as CD11c−, CD68+, F480+. White Pulp Mϕs as CD11c−, CD68+, F4/80−. Marginal Zone Mϕs as CD11c−, CD68+, SIGNR1+. Metallophilic Mϕs as CD11c−, CD68+, CD169+.

Primary Mϕ isolation

Mϕs were isolated by peritoneal lavage and adhesion to tissue-culture-treated plates. Mϕs were harvested by bone marrow isolation and culturing in L-cell conditioned medium, containing M-CSF, as described before (28).

Cell culture

Special care was taken to cultivate Mϕs in normoglycemic (5.5 mM glucose) conditions in DMEM culture and to carefully monitor medium pH and lactate accumulation. For primary Mϕs, mice were injected with thioglycolate for peritoneal elicitation or after bone marrow isolation and cultured in DMEM and M-CSF and 1 g/L (5.5mM “normal glucose”) with 10% non-heat inactivated FBS. In preliminary studies: J774 cells were cultured in 4.5 g/L (25mM “high glucose”) DMEM with 10% FBS. RAWs were cultured in RPMI. Cells

Author Manuscript Author Manuscript Author Manuscript Author Manuscript

supplemented with 100 U/mL penicillin, 100 ug/mL streptomycin, and 2–10% FBS. Cells were treated with 10 ng/mL LPS (from Sigma-Aldrich).

Hypoxia/Ischemia

Hypoxic incubations (1.0% O_2, 94% N_2, and 5% CO_2) were carried out in a humidified Coy Hypoxic chamber and oxygen assessed by an Oxygen Analyzer. Alternatively, a *Billups-Rothenberg* modulator incubator flushed with 1% O_2, 5% CO_2 and 94% N_2 was utilized. Anoxic conditions (0% O_2, 95% N_2, and 5% CO_2) were achieved in a bugbox. Hydroxylase inhibition and/or stabilization of HIFs was induced by adding Cobolt Chloride/$CoCl_2$ (*Alfa Aesar*) or dimethyloxalylglycine (DMOG) from BIOMOL when indicated. All assays on hypoxic cells were performed within the hypoxic chamber or immediately upon removal to minimize re-oxygenation effects.

Gene knockdown

One day before transfection, bone marrow derived Mϕs were seeded in a 24 well plate at a density of $2.5x10^5$ cells/well, to reach 80% confluency at the time of transfection. Using *Lipofectamine* transfection reagent (*Invitrogen*) in OptiMEM serum-free medium (*Invitrogen*), Mϕs were treated with 10μM pooled siRNA against the *Epas1/Hif-2α* gene (Qiagen, Flexitube siRNA 1027415), *Sod2, Phd3* (Qiagen Flexitube siRNA 1027415), or scrambled control siRNA for 24 hours.

Adenoviral transduction

WT and *Hif-2α −/−* Mϕs were treated with Ad-GFP or Ad-GFP-EPAS (HIF-2α, Vector Biolabs ADV-258542) at 500 MOI for 24 hours followed by incubation with R18 labeled apoptotic Jurkats or fluorescent beads, and engulfment enumerated by microscopy.

In vitro Apoptotic Cell (AC) and particle binding and engulfment assays

Bone marrow derived cells (Mϕs) (isolated initially as $5x10^5$ cells/well in a 24 well non-tissue-culture-treated plate) were incubated with PKH67-GL labeled ACs (1:5 or 1:1 BMDC:AC ratio) for 2 h at 4°C for the binding experiment, and at 37°C for AC-engulfment experiments. Alternatively, Mϕs were overlaid with fluorescent (calcein-AM) apoptotic Jurkat T-cells (UV-induced) vs. fluorescent viable Jurkat T-cells at a ratio of 1:1 or 5:1 for indicated time points and subsequently thoroughly rinsed with cold PBS to remove non-engulfed targets. For microscopy, AC binding experiments were conducted by inhibiting actin cytoskeletal reorganization using cytochalasin D (5μg/mL). The cells were then mounted on a slide and analyzed by fluorescence microscopy to quantify binding and engulfment. Cells on glass coverslips were fixed with 4% paraformaldehyde and were visualized using a phase-contrast microscope (Nikon Eclipse Ti) with a digital camera (Photometrics Coolsnap HQ2). Surface area was measured using *ImageJ* software. Uptake of Alexa Fluor 488 *Escherichia coli* (K-12 strain) BioParticles (Invitrogen, Paisley, United Kingdom) after 30 minutes of co-culture (multiplicity of infection of 1:1) was determined by flow cytometry (FACSCalibur; Becton Dickinson). Alternatively, neutrophils were incubated with opsonized zymosan (0.2–1 mg/mL) for 30 minutes, and the phagocytic index was calculated using microscopy.

Author Manuscript Author Manuscript Author Manuscript Author Manuscript

MitoSox and Mito Tempo treatment

To measure mitochondrial reactive oxygen species, bone marrow-derived Mϕs were loaded with 2.5μM MitoSOX reagent (*Thermo Fisher*) in DMEM media with 10% FBS, incubated for 10 mins at 37°C in the dark, and then rinsed 3X with PBS and imaged. For ROS scavenging, bone marrow-derived Mϕs were treated with 1μM *MitoTempo* (Sigma Aldrich) prior to co-culture with apoptotic Jurkats or polysterene beads for 60 minutes, as described above.

Subcellular fractionation

Hif-2α+/+ and *Hif-2α−/−* Mϕs were gently lifted, pelleted, and suspended in 500μl hypotonic solution containing 20mM Tris-HCL, 10mM NaCl, 3mM $MgCl_2$, pH 7.4, and incubated on ice for 15 minutes. 25μL of 10% NP-40 was added, and the nuclear fraction was pelleted by centrifugation for 10mins at 3000 RCF. Supernatant containing the cytoplasmic fraction was removed and the nuclear pellet was suspended in RIPA buffer containing protease inhibitor cocktail. Lysates were probed for NRF2. Cells were treated with 100mM H_2O_2 as positive control for NRF2 nuclear localization. Alternatively, nuclear proteins were isolated using the NE-PER nuclear extraction kit (Thermo Scientific, Rockford, IL).

Immunoblots

For HIF-2α: Lysis Buffer was added to culture dishes and incubated on ice for 10 minutes. RIPA buffer consists of 25 ml of 1M TRIS-HCL, 5ml NP-40, 1.5g Na-deoxycholate, 15ml 5M NaCl, 1ml 0.5 M EDTA, 5ml 10%SDS, and 1x proteinase inhibitor cocktail. Alternatively, cells were dounce homogenized and passed through a 27-gauge needle several times in lysis buffer containing Tris, EDTA, sucrose, and protease inhibitor. Samples were collected and debris spun down to collect supernatant. After measuring protein concentration, 6x laemmli buffer with mercaptoethanol was added to a final 2% concentration. Samples were vortexed then boiled for 10 minutes and then vortexed again before loading. After Western transfer, blots were blocked with 5% milk in TBST for 1h RT, then incubated in primary anti-HIF-2α (*Novus* NB100-122, 2 ug/ml) in milk in TBST at 4C overnight. Blots were rinsed 3x for 10 mins in TSBT then incubated with secondary antibody for 1.5h at 4C.

Chromatin Immunoprecipitation

Chromatin for ChIP was prepared using a commercially available kit (*Millipore#17-600*) from WT and *Hif-2α−/−* Mϕs by fixing the cells in 1% formaldehyde for 10 minutes in a petri dish, followed by quenching with glycine. Cells were extracted in lysis buffer containing protease inhibitors and then sonicated for 6 cycles of 15 seconds each, resting on ice for 50 seconds between each cycle. Cross-linked chromatin was incubated overnight with 5μg of antibodies against HIF-2α, NRF2, or control IgG. Samples from 3 immuno-precipitations were used. Samples were used as template for RT-PCR. PCR primers were designed to amplify a 300bp region of the *Marco* promoter containing predicted NRF2 binding site, as well as promoter (PRM) and enhancer (ENC) regions. ChIP primers as follows: **PRM1-F:** CTG CAC CGG TTC TCT TCC AA. **R:** TCC TGT TGC AGC ATC

Author Manuscript Author Manuscript Author Manuscript Author Manuscript

GTT CT. **PRM2-F:** CCA CAG GTT CAA CAG GGA CA. **R:** TGC CTC TTT GCA GCA TAC CA. **PRM3-F:** AGG GAT ACC TGT CCC TGT CC. **R:** AAA GTG CAC ATC AGG CAA GC. **ENC1-F:** GGC ACT CAG TGT GCT GGT TA. **R:** TGA GAC TCC TCT CGG GTT GT. **ENC2-F:** CTG TGG TTG TTG CGC AGA TT. **R:** GCA TGC CCA CAG ACC AAA CTA. **ENC3-F:** CAC TGA CCC AGC ATT GCC TC. **F:** AGC CAG GGG AGA GAT TTG TTT **ARE-F:** TCC TCA CAG ATA TGG AGC TC. **R:** TCT GCT TGC TGC CTA GAG GT.

Assays of mRNA stability

WT and *Hif-2α* −/− Mϕs were plated in 6 well plates, media was replaced with1g/L glucose DMEM with 10% FBS containing 10μg/mL Actinomycin D (Sigma A9415). *Marco* mRNA was quantified relative to 18S rRNA at various times following Actinomycin D treatment. RNA was extracted from cells using TRIZOL (Thermo Fisher) and RNA species were detected by RT-PCR as described previously. RNA half-life was calculated by linear regression analysis.

Primers used for qPCR analysis

The forward and reverse primers for *Tnf-α* were CGG AGT CCG GGC AGG T and GCT GGG TAG AGA ATG GAT GAA CA, respectively. 36B4 was used as the internal control. The forward and reverse primers for 36B4 were AGA TGC AGC AGA TCC GCA T and GTT CTT GCC CAT CAG CAC C, respectively. *Hif-1α-F*: GTT TAC TAA AGG ACA AGT CAC C (29). *Hif-1α-R*: TTC TGT TTG TTG AAG GGA G, *Vegf-F*: TGC CAA GTG GTC CCA G, *Vegf-R*: GTG AGG TCT TGA TCC G, *Ifn-γ* ChIP F: CTC ATC GTC AGA GAG CCC AA, *Ifn-γ* ChIP R: AGG ATC AGC TGA TGT GTC TT. Total RNA was extracted from Mϕs using the RNeasy kit (Qiagen). cDNA was synthesized from 4 μg of total RNA using oligo (dT) and Superscript II (*Invitrogen*). cDNA was subjected to quantitative RT-PCR amplification using a SYBR Green PCR Master Mix (*Applied Biosystems*). The reactions were run on a MX4000 multiplex quantitative PCR system (*Stratagene*). Additional oligonucleotides utilized for semi-quantitative/real-time PCR: ***Tyro*** **F**: CAG GGC TAA AGG TCG TCT CC. **R**: ATG TCC ACCATG AAC CGG AC. ***Axl*** **F**: CAT ATC GAG GCC AGG ACA CC. **R**: ATC CCC AGC CGA GGT ATA GG. ***Mertk*** **F**: GAG GAC TGC TTG GAT GAA CTG TA. **R**: AGG TGG GTC GAT CCA AGG. ***Cd36*** **F**: TCC TCT GAC ATT TGC AGG TCT ATC. **R**: AAA GGC ATT GGC AAG AA. ***Marco*** **F**: TCC CAG GTC TTG TAG GCA GA. **R**: TAA CCG AGC ATG CGA CAG AA. ***Sra*** **F**: GGC TGG AGG GAA GTT GTC AAT AC. **R**: CCA CTG GTG ATG TAA AAG TTC TTG. **Nrf2 F**: TCT CCT CGC TGG AAA AAG AA. **R**: AAT GTG CTG GCT GTG CTT TA. **18S F**: GTA ACC CGT TGA ACC CCA TT. **R**: CCA TCC AAT CGG TAG TAG CG. **Gpx1 F**: TCG GAC ACC AGG AGA ATG GCA. **R**: GAG CGC AGT GGG GTC GTC AC. **Cas1 F**: GCA TCG AGC CCA GCC CTG AC. **R**: TTG GGG GCA CCA CCC TGG TT. **Sod1 F**: GAG ACC TGG GCA ATG TGA CT. **R**: TTG TTT CTC ATG GAC CAC CA. ***Sod2*** **F**: TCA ATG GTG GGG GAC ATA TT. **R**: GAA CCT TGG ACT CCC ACA GA. ***Ccs*** **F**: GCC TGG TTA TCG ATG AGG GG. **R**: CAA TGA TGC CAC AGG CCA AC. ***Prdx1*** F: TTG GCG CTT CTG TGG ATT CT. **R**: GGT GCG CTT GGG ATC TGA TA. ***Nox1*** F: CCT TCC ATA AGC TGG TGG CA. **R**: GGC CTG TTG GCT TCT TCT GTA G. ***Txnrd*** **F**: GCT

Author Manuscript Author Manuscript Author Manuscript Author Manuscript

GAG CAC ATT GTC ATT GC. **R**: TCC AAC CAC CAA CGT TTT CC. ***Mpo*** **F**: ATG CAG TGG GGA CAG TTT CTG. **R**: GTC GTT GTA AGA TCG GTA CTG.

Statistical Analysis and bioinformatics

Bioinformatics - Transcription factor binding sites were predicted using Matinspector (http://www.genomatix.de/cgi-bin/matinspector). Data were analyzed using Prism 5.0 software (GraphPad Software, San Diego, CA) using unpaired, 2- tailed *t-tests* for comparisons between 2 groups and 1-way or 2-way analysis of variance (ANOVA; with Bonferonni post-test adjustment) for other data as appropriate. Significance was accepted when $p < .05$. Data are expressed as mean ± standard error of the mean (SEM).

Results

Hif-2α is not required for efferocytosis during hypoxia, however Hif-2α-deficient macrophages (Mϕs) engulf apoptotic cells more efficiently under non-hypoxic (20% O_2) incubation

We began by directly testing requirements for *Hif-2α* during Mϕ efferocytosis. *Hif-2α floxed (fl)* mice were crossed to *LysMcre* and bone marrow-derived Mϕs incubated at 1% oxygen in temperature and humidity controlled chambers. Under these conditions, *Hif-2α*$^{fl/fl}$ *LysMcre* Mϕs exhibited >90% reduction of HIF-2α protein. When cultures were subsequently co-cultivated with apoptotic cells, *Hif-2α* was not required for efferocytosis under hypoxic conditions (Fig. 1A), unlike for *Hif-1α* (Fig. 1B) (21). Surprisingly, examination of Mϕs from *Hif-2α*$^{fl/fl}$ *LysMcre* mice under control conditions, exhibited heightened efferocytosis efficiency when incubated under normal atmospheric (20% O_2) incubators (Fig. 1C). Importantly, the degree of change in uptake is consistent with the delta of known physiologic modulators of efferocytosis (30). Special care was taken to ensure assays were performed under sub-confluent conditions and in fresh normo-glycemic medium to prevent potential metabolic activation of HIFs. We also utilized gas-permeable plates to confirm increased efferocytosis under non-hypoxic, pimonidazole-negative (31) tissue culture conditions (Fig. 1D). Low levels of HIFs have previously been shown to be expressed under conditions classified as normoxic (32) and consistently, western blots revealed ~10% HIF-2α levels from normoxic Mϕs, relative to their hypoxic counterparts (Fig. 1E). Indeed, titration of *Hif-2α*$^{fl/fl}$ gene dose in the background of either heterozygous or homozygous *LysMcre*, revealed that efferocytosis efficiency inversely correlated with HIF-2α levels (Fig. 1E **graph**). Enhanced efferocytosis after acute knockdown of *Hif-2α* was consistent with direct actions of HIF-2α, as opposed to compensatory mechanisms during Mϕ differentiation in culture (Fig. 1F). Also, Mϕs simultaneously lacking both HIF-α isoforms were better efferocytes, indicating HIF-1α was not working in a compensatory manner in *Hif-2α*$^{-/-}$ Mϕs (Fig. 1G). This phenotype was specific to the *Hif-2α* isoform, as *Hif-1α* deficient Mϕs did not reveal statistically significant elevations in engulfment.

HIF-2α is sufficient to suppress efferocytosis

To address if HIF-2α could independently suppress efferocytosis, we first knocked down negative-regulator of HIFs, prolyl hydroxylase domain-3, or *Phd-3*. Prolyl hydroxylation promotes HIF association with von Hippel-Lindau (pVHL) ubiquitin E3 ligase and

Author Manuscript Author Manuscript Author Manuscript Author Manuscript

destruction by the ubiquitin-preoteasome pathway (8). PHD3 has also been reported to be partially selective for HIF-2α (33). As shown in Fig. 2A, *Phd-3* silencing in normoxic primary Mϕs both elevated HIF-2α protein levels, as well as suppressed efferocytosis efficiency. Suppressed efferocytosis was not due to a general cellular toxicity, as Mϕs with heightened HIF-2α were equally competent at phagocytosis of control latex beads. Direct targeting of HIF-2α by adenoviral over-expression after transduction, also led to increased HIF-2α and suppressed efferocytosis (Fig. 2B); this was not seen after adenoviral transduction with HIF-1α (*data not shown*). Mϕs from transduced cells also showed enhanced expression of the HIF-2α target gene *Pai1* (*data not shown*). As further corroborating evidence, primary Mϕs from LysMcre *Hif-2α LSL/LSL* mice, which express heightened levels of HIF-2α relative to control (24, 25), also exhibited reduced efferocytosis (Fig. 2C).

Screening of engulfment pathways +/− Hif-2α and identification of a Hif-2α-Marco axis

We next sought to identify the molecular mechanism responsible for enhanced efferocytosis in *Hif-2α fl/fl, LysMcre* Mϕs. We executed a screen of receptors and signaling pathways involved in phagocytosis and measured mRNA expression by qRT-PCR from *Hif-2α fl/fl vs. Hif-2α fl/f LysMcre* Mϕs. As shown in Fig. 3A, analysis of *Marco* (34) gene expression revealed a specific and >10 fold induction in the absence of *Hif-2α*. Impressively, the reverse phenotype was found after inducing *Hif-2α* after *Phd3* knockdown. Normoxic alterations in mRNA were recapitulated at the protein level (Fig. 3B & C). Furthermore, direct adenoviral transduction of HIF-2α also reduced MARCO (Fig. 3D). Elevations of Marco mRNA in *Hif-2α fl/fl LysMcre* Mϕs were corroborated by surface staining for MARCO by flow cytometry (Fig. 3E). Because *Marco* mRNA is known to be induced by LPS, special care was taken to avoid lipopolysaccharide contamination by measuring and confirming absence of endotoxin contamination via LAL assays.

MARCO is required for enhanced efferocytosis in the absence of HIF-2α

To test requirements for MARCO during efferocytosis in *Hif-2α −/−* Mϕs, MARCO was blocked by administration of a monoclonal antibody, specific to its ectodomain (clone ED31). As shown in Figure 3F, MARCO blocking antibody effectively abrogated efferocytosis enhancements. Consistently, *Hif-2α* knockdowns in Mϕs from *Marco −/−* mice did not exhibit enhanced efferocytosis relative to control (Fig 3G).

MARCO transcription is elevated in the absence of Hif-2α

Accumulation of MARCO could result from increases in mRNA transcription, stability, mRNA translation, or protein stability. To determine if *Marco* mRNA was post-transcriptionally stabilized in the absence of *Hif-2α*, transcription in primary Mϕs was blocked with Actinomycin D (ActD) and mRNA levels measured by qRT-PCR. *Marco* mRNA stability was unchanged by *Hif-2α* deficiency as the percentage of initial *Marco* message was 71% in $Hif\text{-}2\alpha^{fl/fl}$ vs. 73% in $Hif\text{-}2\alpha^{fl/fl}$ *LysMcre* Mϕs, following ActD treatment (Sup. Fig. 1A). HIF-2α enhancement was determined to likely be transcriptional, as aryl hydrocarbon nuclear translocator (*Arnt*) deficient Mϕs also exhibited enhanced efferocytosis (Sup. Fig. 1B). Finally, *Hif-2α* knockdown failed to increase efferocytosis in the $Arnt^{fl/fl}$ *LysMcre* Mϕs (Sup. Fig. 1C).

Author Manuscript Author Manuscript Author Manuscript Author Manuscript

Transcriptional regulation of MARCO by HIF-2α occurs through NRF2

To ascertain whether the *Marco* gene is a transcriptional target of HIF-2α, we first analyzed the mouse genomic sequence in the 5′ un-translated region (UTR) of *Marco* (Fig. 4A). *In silico* analysis of FASTA gene sequences revealed the lack of conserved RCGTG motif hypoxic response elements/HREs, as well as so called inhibitory reverse HREs (35), hundreds of base pairs upstream of the *Marco* transcription start site, respectively. HIFs have also been found to bind to enhancer regions, for example USF2 is a HIF-2α binding partner at EBOX enhancer regions, proximal to hypoxia responsive genes (36). Therefore, we next tested if HIF-2α might negatively regulate transcription of *Marco* through affecting promoter or enhancer occupancy and performed chromatin immune-precipitation as previously described (37). In contrast to HIF-2α binding to control *Vegf* promoters during hypoxia, relatively low amounts of HIF-2α binding to the MARCO promoter was identified after using probes scanning the promoter region 2kb upstream of the MARCO transcription start site, as well as three reported MARCO-associated enhancer regions (Fig. 4B).

Marco is a target of nuclear factor (erthroid-derived 2)-like 2 (NFE2L2 or Nrf2)(37) and the *Marco* promoter contains an antioxidant response elements (ARE). We therefore next looked for enhanced NRF2 binding to *Marco.* Indeed, absence of *Hif-2α* markedly enhanced NRF2 association with the *Marco* ARE (Fig. 4C). Consistent with elevated NRF2-binding, *Hif-2α-deficiency* also led to increased NRF2 in the nucleus and activation of NRF2 target genes (38) (Fig. 4D). To determine if *Nrf2 is required for enhanced efferocytosis in Hif-2α-deficient* phagocytes, we used siRNA to reduce *Nrf2* (>90% reduction) and MARCO in *Hif-2α fl/fl LysMcre* Mϕs, and as expected, reversed the enhanced efferocytosis phenotype (Fig. 4E). Finally, direct agonism of NRF2 with sulforaphane (39) increased both MARCO and efferocytosis (Fig. 4F).

Hif-2α deficient Mϕs produce heightened mROS to activate NRF2, Marco gene expression, and efferocytosis

In light of the activation of NRF2 in *Hif-2α-deficient* Mϕs, we next measured markers of ROS. Gene expression profiling revealed significant reductions in antioxidant gene expression, including catalase, glutathione peroxidase, and superoxide dismutase (Sup. Fig. 2A–B). The reduction of multiple antioxidant mRNAs suggested a generalized mechanism of cellular ROS control, beyond the scope of this study, but also supported by other studies (40). Consistent with our findings, knockdown of antioxidant *Sod2* also increased MARCO and efferocytosis (Sup. Fig. 2C). Given the link between mROS and HIFs (41), we next utilized mitochondrial superoxide indicators to measure mitochondrial-localized ROS levels in *Hif-2α* deficient Mϕs. Indeed *Hif-2α* deficient Mϕs exhibited on average a greater than 2-fold elevation in mitoSOX signal (Fig. 5A). The mROS scavenger, *mitoTEMPO*, not only inhibited mROS as expected, but also restored MARCO and efferocytosis (Fig. 5B&C). In support of a role fpr mitochondrial-derived ROS, *Tfam-deficient* Mϕs (42) were unable to promote elevated efferocytosis after adding *Hif-2α* siRNA (Sup. Fig. 3).

Author Manuscript Author Manuscript Author Manuscript Author Manuscript

Hif-2α deficiency in vivo leads to elevated MARCO levels and enhanced efferocytosis during peritonitis

To test the *in vivo* significance of our findings, we measured MARCO expression levels in *Hif-2α-deficient* mice. We first examined spleen, where marginal zone Mϕs characteristically express MARCO (34). Indeed, splenic Mϕ populations exhibited significantly elevated MARCO levels (Fig. 6A). Splenic Red Pulp, Metallophilic, White Pulp, and Marginal Zone resident Mϕs were analyzed for MARCO surface expression by flow cytometry. After quantification, all 4 of the Mϕ subsets showed elevated MARCO expression in *Hif-2α-deficient* spleens (Fig. 6B). Remarkably, this phenotype was reversed in $Hif\text{-}2\alpha^{LSL/LSL}$ *LysMcre mice, which express elevated HIF-2a relative to control* (24, 25).

To test the role of HIF-2α during *in vivo* efferocytosis, we injected apoptotic cells and measured percent uptake by flow cytometry (43) in peritoneum. It is important to note that the redundancy of apoptotic cell engulfment receptors is a likely reason why single receptor deficiency does not lead to clearance defects under steady state. Therefore, $Hif\text{-}2\alpha^{fl/fl}$ and $Hif\text{-}2\alpha^{fl/fl}$ *LysMcre* mice were challenged with apoptotic thymocytes through intraperitoneal injection, following administration of MARCO blocking antibody ED31 or IgG1 isotype control. Similar to the *in vitro* findings, peritoneal Mϕs isolated by peritoneal lavage from *Hif-2α* deficient mice had higher MARCO levels and a higher percentage of internalized apoptotic targets, indicating enhanced efferocytosis, which was dependent on MARCO (Fig. 7A–B).

We hypothesized that an mROS-HIF-2α-MARCO axis might be particularly important during pro-inflammatory bacterial responses. We linked studies implicating ROS and separately, MARCO, to antibacterial recognition of bacteria (44, 45). We first asked whether *Hif-2α*-deficient Mϕs exhibited an increased capacity for *in vivo* bacterial phagocytosis, in a MARCO-dependent manner. This was tested after peritoneal injection of gram-positive *Staphyloccus Aureus* into $Hif\text{-}2\alpha^{fl/fl}$ and $Hif\text{-}2\alpha^{fl/fl}$ *LysMcre* mice. Similar to apoptotic cells, *Hif-2α*-deficient Mϕs were more efficient at MARCO-dependent bacterial phagocytosis (Fig. 7C) and exhibited reduced plasma inflammatory cytokines, including IL-1β. Importantly, reductions in IL-1β were inhibited with the addition of MARCO-blocking antibodies (Fig. 7D).

Beyond genetic targeting, we importantly asked if natural *Hif-2α* regulators might also affect *Marco,* through HIF-2α. Previous reports indicate that Th2 cytokine IL-4 increases HIF-2α (46). Others have shown that IL-4 can down-regulate *Marco* expression (47) and separately, IL-4 can inhibit bacterial clearance (48). To test requirements for *Hif-2α*-regulation of *Marco* in the presence of IL-4, $Hif\text{-}2\alpha^{fl/fl}$ and $Hif\text{-}2\alpha^{fl/fl}$ *LysMcre* mice were injected IP with IL-4 *vs.* vehicle control. Subsequently, IP-injections included fluorescently labeled gram-positive *S. aureus* at equivalent bacteria: Mϕ multiplicities of infection/MOIs for each genotype. Peritoneal Mϕs were lavaged and phagocytosis was quantified by flow cytometry. Flow plots (Fig. 7E) revealed that under saturating conditions, IL-4 significantly decreased the levels of *S. Aureus* (FITC) positive Mϕs, and impressively, this required *Hif-2α*. Thus, natural induction of HIF-2α-MARCO, such as though IL-4, in turn suppresses bacterial clearance capacity. Taken together, a picture of HIF-2α as significant negative regulator of Mϕ phagocytic activation emerges.

Author Manuscript Author Manuscript Author Manuscript Author Manuscript

Discussion

Herein we uncover a novel role for HIF-2α in the suppression of Mϕ phagocytic activation. Interestingly, this can occur under non-hypoxic culture conditions and at cellular steady state. Even at low expression levels, relative to hypoxia, (Fig. 1), HIF-2α functions to suppress key Mϕ signaling pathways, including mitochondrial ROS (mROS)(49) (Figure 5) and MARCO-dependent phagocytosis (34) (Figure 3). From the data, we have outlined a working model (Sup. Fig. 4) where basal levels of Mϕ HIF-2α, escape PHD-driven prolyl hydroxylation (8, 50) to drive transcription of antioxidant genes, potentially SOD2 (40) (Sup. Fig. 2). Redox suppression by HIF-2α is necessary to maintain a quiescent Mϕ phagocytic state, and this occurs via blockade of an mROS-*Marco* signaling axis (Fig. 5 & Sup. Fig. 2). Because the effect of HIF-2α on *Marco* is through mROS, indeed other mROS-responsive pathways, beyond the scope of this study, may likely be responsive. Nevertheless, the importance of MARCO surfaces in that it is uniquely sensitive to mROS escalations, in contrast to other phagocytosis receptors (Fig. 3A). Also according to the model, Toll Like Receptor/TLR activation of mROS (51), for example during bacterial infection (Fig7) or after LPS (Sup. Fig. 4E), is predicted to overwhelm baseline HIF-2α antioxidant control, thereby providing a mechanism to quickly and specifically mobilize NFR2 to the *Marco* promoter (52). Such a rapid response may be applicable at times of acute bacterial challenge, where resting/resident Mϕs, which predominantly express homeostatic apoptotic cell-specific Tim4 and MERTK phagocytic receptors (53), require rapid mobilization of bacteria-biased MARCO. Besides basal HIF-2α function under normoxia or “mild” hypoxia, HIF-2α can also be induced by IL-4 (Sup. Fig. 4F) (46) to further reduce mROS and *Marco*. This working model is consistent with HIF-2α as significant negative regulator of Mϕ phagocytic activation.

Our normoxic findings, though contrary to initial expectations, are supported by other studies of HIF in non-hypoxic conditions (54–56). For example, HIF-1α is stabilized in circulating hematopoietic stem cells, independent of oxygen tension (57); this occurs in part through down-regulation of HIF ubiquitin ligase von Hippel-Lindau (VHL) protein. Also, changes in HIF transcription, after IL-4 treatment for example, have been shown to alter HIF protein levels, independent of post-translational degradation by HIF-targeting VHLs (58) (59). In Mϕs, an oxygen-independent calcineurin-NFAT-HIF-1α axis is activated by sphingosine-1-phosphate, which can be found in the supernatants of neighboring apoptotic cells (60). Furthermore, most normoxic studies of Mϕ HIFs have been conducted after inflammatory stimulation, including post TLR ligation (12, 13, 15). Our findings are unique in that Mϕ HIF-2α-regulation of MARCO occurs at steady state and in the absence inflammatory triggers.

In contrast to normoxic phagocytic activity, HIF-2α does not affect phagocytosis under hypoxia (Figure 1). Given that hypoxic induction of HIFs dramatically alters gene expression profiles of multiple Mϕ effector networks in primary and human Mϕs (61), it is not surprising that the HIF-2α-MARCO axis is lost to other competing signaling pathways under hypoxia. *In our hands, Marco* expression is induced under hypoxia, independent of HIFs. Also, data mining from previously published array analyses suggests that MARCO, in primary human monocytes, may be induced ~2fold after 16 hours in 1% oxygen (62). One

Author Manuscript Author Manuscript Author Manuscript Author Manuscript

explanation for this might be hypoxic-mitochondrial mROS signaling (41), which can act independent of HIFs, and in turn is predicted to drive nuclear translocation of NRF2 onto the *Marco* promoter (Fig. 4).

In contrast to *Hif-2α*, *Hif-1α* is required for hypoxic-induced phagocytosis (21). Furthermore, HIF-1α in Mϕs has further been shown to coordinate bacterial killing (17). Although HIF isoforms regulate overlapping functions, they also control independent and potentially counteracting pathways (63). For example, HIF-1α uniquely regulates the Mϕ "M1" polarization phenotype (18) (64) (65), in part through HIF-1α control of glycolytic enzyme expression and the glucose transporter GLUT-1 (66, 67). In contrast, HIF-2α appears to act independent of glycolytic control, instead focused to endotoxin-induced cytokine production (19). HIF-2α is also linked to Mϕ alternative activation (46) (68) and is induced by Th2 cytokines, including IL-4 (46) and can oppose the pro-inflammatory action of HIF-1α (46, 69, 70). Our findings add a new tangent to these described HIF isoform dichotomies, wherein reduced oxygen acts as the molecular threshold to supersede HIF-2α phagocytic suppression, in favor of an opposing and dominant hypoxic HIF-1α pro-phagocytic pathway.

To the best of our knowledge, the link between HIFs and MARCO has not been described in the literature. This is understandable, as our *in silico* analysis of *Marco* gene regulatory regions uncovered a paucity of hypoxic response elements/HREs, relative to other known HIF targets. Though studies have linked HIFs to induction of phagocytosis receptors, there interestingly are reports of phagocytic receptor suppression by hypoxia, reinforcing the interesting concept of differential hypoxic or HIF regulation of Mϕ phagocytosis receptors. For example, reductions in scavenger receptors *Sra* and *Cd36* during hypoxia have been published and are seemingly *Hif*-independent in Mϕ RAW cell lines (71). In contrast, others find requirements for *Hif-1α* in *Sra* suppression (72). *Sluimer et al.* found reductions in *Mertk* in the context of atherosclerosis (73), as has our group (unpublished studies). As described in our working model, our findings during normoxia indicate that HIF-2α regulates *Marco* indirectly, although through activation of a specific ROS-sensitive NRF2-Marco axis (Fig. 4). In contrast to MARCO, the scavenger receptor *Cd36* is transcriptionally induced during hypoxia by HIF-1α to increase phagocytic uptake (21). Interestingly, transglutaminase 2, which has also been implicated in phagocytosis (74), has been shown to directly interact with Hif-1β, thereby suppressing Hif-1α signaling (75). Also, hypoxia has been shown to induce epithelial CD55 at mucosal surfaces, and this promoted clearance of apical PMNs in the gut (76). *Ongoing studies are examining HIF-2α association with other candidate phagocytosis genes by ChipSeq*.

In the arena of the phagocytic regulation *per se*, it is interesting to note that far fewer homeostatic negative regulators of phagocytosis have been described, relative to pro-phagocytic stimuli, the latter of which often culminate in the modulation of Rho GTPases and assembly of filamentous actin at the phagocytic cup. Natural inhibitors of phagocytosis include Sec22, which negatively regulates levels of SNARE/fusion proteins (77). Again, although the mechanism of HIF-2α inhibition of phagocytosis is indirect, this pathway nonetheless is specific to *Marco*.

Author Manuscript Author Manuscript Author Manuscript Author Manuscript

Numerous links between HIFs and ROS have been made, including seminal findings during hypoxia, linking ROS from mitochondrial complex III (41) and independent of oxidative phosphorylation (78), to stabilization of HIF-1α. In the case of *Hif-2α*, mice that lack one copy of Hif-2α (79) exhibit a mitochondrial disease state. For example, *Hif-2α-deficient* livers are under elevated oxidative stress and express reduced levels of *Sod2* (40), the latter of which is consistent with findings in adrenal glands (80), and our new findings in Mϕs. Our gene expression analyses suggest HIF-2α positive regulation of a number of other antioxidant enzymes, including glutathione peroxidase (GPX1), thioredoxin reductase (TXNRD1), and myeloperoxidase (MPO) (Sup. Fig. 2). This hints that HIF-2α may interestingly function as a master regulator of cellular oxidative state in Mϕs. Separately, NRF2 has been linked to phagocytosis. For instance and in Mϕs, neutrophil oxidative-burst byproducts, i.e., heme oxygenase, have been shown to induce NRF2 and lead to increased efferocytosis of apoptotic neutrophils (81). At the level of phagocytosis receptors, previous studies have linked MARCO to activation by ROS (37). Also, cellular oxidative stress caused by hypoxic incubation has been shown to modulate the expression of other Mϕ efferocytosis receptors, including CD36 (21). Taken together, our data and the literature suggest a conserved link between HIFs, ROS, and phagocytosis.

Particular aspects of the study should not be over-interpreted. For example, although *Hif-2α* deficiency enhances bacterial clearance through MARCO, this does not lead us to suggest targeting HIF-2α as an antibacterial approach. Rather, this pathway may partially explain compromised bacterial surveillance (48) during Th2/IL-4 associated parasitic infections, which would be predicted to have a heightened ratio of HIF-2α to MARCO. Another potentially relevant pathophysiology may occur during obesity, where it has been demonstrated that M2-classified Mϕs express high levels of HIF-2α in the adipose tissue of obese mice (70); the role of MARCO during obesity is unclear.

Multiple questions remain. Future studies are necessary to test the significance of the HIF-2α: *Marco* axis in human Mϕs, as has been done for HIF-2α in neutrophils (82). Also of interest is the complete range of basal HIF-2α activity in phagocytes under steady state, which has not been conclusively characterized. Besides steady state, the link between IL-4, HIF-2α, and alternatively activated or M2-polarized Mϕs (46), further raises questions during wound healing. For example, HIF-2α in M2 Mϕs may promote inflammation resolution, in part through suppression of pro-inflammatory mROS and MARCO signaling pathways. Finally, and consistent with other homeostatic feedback circuits, it will be interesting to determine if MARCO-mediated phagocytosis signals-back to regulate HIF-2α, during the return to a resting Mϕ phenotype, or even with aging-associated elevations in ROS.

Supplementary Material

Refer to Web version on PubMed Central for supplementary material.

Acknowledgments

Thank you to *Y. Shah* for LSL-HIF mice. Thank you to *F. Gonzalez* for ARNT mice.

Author Manuscript Author Manuscript Author Manuscript Author Manuscript

Funding: These studies were supported by NIH R01HL122309 to ET and CLIMB, CMBD, and an NIH Diversity Supplement (R01HL122309) to SD. National Institute of Health Grants R01 DK097075, R01-HL092188, R01-HL098294, POI-HL114457, and R01-HL119837 to HKE.

References

1. Medzhitov R. Origin and physiological roles of inflammation. Nature. 2008; 454:428–435. [PubMed: 18650913]
2. Gordon S. The macrophage: past, present and future. Eur J Immunol. 2007; 37:S9–17. [PubMed: 17972350]
3. Nathan C. Immunology: Oxygen and the inflammatory cell. Nature. 2003 Apr 17; 422(6933):675–6. [PubMed: 12700748]
4. Eltzschig HK, Carmeliet P. Hypoxia and inflammation. N Engl J Med. 2011; 364:656–665. [PubMed: 21323543]
5. Nizet V, Johnson RS. Interdependence of hypoxic and innate immune responses. Nature reviews Immunology. 2009; 9:609–617.
6. Semenza GL. Hypoxia-inducible factors in physiology and medicine. Cell. 2012; 148:399–408. [PubMed: 22304911]
7. Wang GL, Semenza GL. General involvement of hypoxia-inducible factor 1 in transcriptional response to hypoxia. Proc Natl Acad Sci U S A. 1993; 90:4304–4308. [PubMed: 8387214]
8. Jaakkola P, Mole DR, Tian YM, Wilson MI, Gielbert J, Gaskell SJ, von Kriegsheim A, Hebestreit HF, Mukherji M, Schofield CJ, Maxwell PH, Pugh CW, Ratcliffe PJ. Targeting of HIF-alpha to the von Hippel-Lindau ubiquitylation complex by O2-regulated prolyl hydroxylation. Science. 2001; 292:468–472. [PubMed: 11292861]
9. Wang GL, Jiang BH, Rue EA, Semenza GL. Hypoxia-inducible factor 1 is a basic-helix-loop-helix-PAS heterodimer regulated by cellular O2 tension. Proc Natl Acad Sci U S A. 1995; 92:5510–5514. [PubMed: 7539918]
10. Wenger RH, Stiehl DP, Camenisch G. Integration of oxygen signaling at the consensus HRE. Sci STKE. 2005:18.
11. Ishida I, Kubo H, Suzuki S, Suzuki T, Akashi S, Inoue K, Maeda S, Kikuchi H, Sasaki H, Kondo T. Hypoxia diminishes toll-like receptor 4 expression through reactive oxygen species generated by mitochondria in endothelial cells. J Immunol. 2002; 169:2069–2075. [PubMed: 12165534]
12. Ramanathan M, Luo W, Csoka B, Hasko G, Lukashev D, Sitkovsky MV, Leibovich SJ. Differential regulation of HIF-1alpha isoforms in murine macrophages by TLR4 and adenosine A(2A) receptor agonists. J Leukoc Biol. 2009; 86:681–689. [PubMed: 19477908]
13. Peyssonnaux C, Cejudo-Martin P, Doedens A, Zinkernagel AS, Johnson RS, Nizet V. Cutting edge: Essential role of hypoxia inducible factor-1alpha in development of lipopolysaccharide-induced sepsis. J Immunol. 2007; 178:7516–7519. [PubMed: 17548584]
14. Ghosh S, Baltimore D. Activation in vitro of NF-kappa B by phosphorylation of its inhibitor I kappa B. Nature. 1990; 344:678–682. [PubMed: 2157987]
15. Rius J, Guma M, Schachtrup C, Akassoglou K, Zinkernagel AS, Nizet V, Johnson RS, Haddad GG, Karin M. NF-kappaB links innate immunity to the hypoxic response through transcriptional regulation of HIF-1alpha. Nature. 2008; 453:807–811. [PubMed: 18432192]
16. Walmsley SR, Print C, Farahi N, Peyssonnaux C, Johnson RS, Cramer T, Sobolewski A, Condliffe AM, Cowburn AS, Johnson N, Chilvers ER. Hypoxia-induced neutrophil survival is mediated by HIF-1alpha-dependent NF-kappaB activity. The Journal of experimental medicine. 2005; 201:105–115. [PubMed: 15630139]
17. Peyssonnaux C, Datta V, Cramer T, Doedens A, Theodorakis EA, Gallo RL, Hurtado-Ziola N, Nizet V, Johnson RS. HIF-1alpha expression regulates the bactericidal capacity of phagocytes. The Journal of clinical investigation. 2005; 115:1806–1815. [PubMed: 16007254]
18. Cramer T, Yamanishi Y, Clausen BE, Forster I, Pawlinski R, Mackman N, Haase VH, Jaenisch R, Corr M, Nizet V, Firestein GS, Gerber HP, Ferrara N, Johnson RS. HIF-1alpha is essential for myeloid cell-mediated inflammation. Cell. 2003; 112:645–657. [PubMed: 12628185]

Author Manuscript Author Manuscript Author Manuscript Author Manuscript

19. Imtiyaz HZ, Williams EP, Hickey MM, Patel SA, Durham AC, Yuan LJ, Hammond R, Gimotty PA, Keith B, Simon MC. Hypoxia-inducible factor 2alpha regulates macrophage function in mouse models of acute and tumor inflammation. The Journal of clinical investigation. 2010; 120:2699–2714. [PubMed: 20644254]
20. Zhang S, Dehn S, DeBerge M, Rhee KJ, Hudson B, Thorp EB. Phagocyte-myocyte interactions and consequences during hypoxic wound healing. Cell Immunol. 2014; 291:65–73. [PubMed: 24862542]
21. Mwaikambo BR, Yang C, Chemtob S, Hardy P. Hypoxia up-regulates CD36 expression and function via hypoxia-inducible factor-1- and phosphatidylinositol 3-kinase-dependent mechanisms. The Journal of biological chemistry. 2009; 284:26695–26707. [PubMed: 19640849]
22. Ortiz-Masia D, Diez I, Calatayud S, Hernandez C, Cosin-Roger J, Hinojosa J, Esplugues JV, Barrachina MD. Induction of CD36 and thrombospondin-1 in macrophages by hypoxia-inducible factor 1 and its relevance in the inflammatory process. PLoS One. 2012; 7:31.
23. Gruber M, Hu CJ, Johnson RS, Brown EJ, Keith B, Simon MC. Acute postnatal ablation of Hif-2alpha results in anemia. Proc Natl Acad Sci U S A. 2007; 104:2301–2306. [PubMed: 17284606]
24. Xie L, Xue X, Taylor M, Ramakrishnan SK, Nagaoka K, Hao C, Gonzalez FJ, Shah YM. Hypoxia-inducible factor/MAZ-dependent induction of caveolin-1 regulates colon permeability through suppression of occludin, leading to hypoxia-induced inflammation. Mol Cell Biol. 2014; 34:3013–3023. [PubMed: 24891620]
25. Kim WY, Safran M, Buckley MR, Ebert BL, Glickman J, Bosenberg M, Regan M, Kaelin WG Jr. Failure to prolyl hydroxylate hypoxia-inducible factor alpha phenocopies VHL inactivation in vivo. The EMBO journal. 2006; 25:4650–4662. [PubMed: 16977322]
26. Shah YM, Ito S, Morimura K, Chen C, Yim SH, Haase VH, Gonzalez FJ. Hypoxia-inducible factor augments experimental colitis through an MIF-dependent inflammatory signaling cascade. Gastroenterology. 2008; 134:2036–2048. [PubMed: 18439915]
27. Getts DR, Terry RL, Getts MT, Deffrasnes C, Müller M, van Vreden C, Ashhurst TM, Chami B, McCarthy D, Wu H, Ma J, Martin A, Shae LD, Witting P, Kansas GS, Kühn J, Hafezi W, Campbell IL, Reilly D, Say J, Brown L, White MY, Cordwell SJ, Chadban SJ, Thorp EB, Bao S, Miller SD, King NJC. Therapeutic Inflammatory Monocyte Modulation Using Immune-Modifying Microparticles. Science Translational Medicine. 2014; 6:219ra217.
28. Wan E, Yeap XY, Dehn S, Terry R, Novak M, Zhang S, Iwata S, Han X, Homma S, Drosatos K, Lomasney J, Engman DM, Miller SD, Vaughan DE, Morrow JP, Kishore R, Thorp EB. Enhanced efferocytosis of apoptotic cardiomyocytes through myeloid-epithelial-reproductive tyrosine kinase links acute inflammation resolution to cardiac repair after infarction. Circulation research. 2013; 113:1004–1012. [PubMed: 23836795]
29. Acosta-Iborra B, Elorza A, Olazabal IM, Martin-Cofreces NB, Martin-Puig S, Miro M, Calzada MJ, Aragones J, Sanchez-Madrid F, Landazuri MO. Macrophage oxygen sensing modulates antigen presentation and phagocytic functions involving IFN-gamma production through the HIF-1 alpha transcription factor. J Immunol. 2009; 182:3155–3164. [PubMed: 19234213]
30. Fadok VA, Bratton DL, Konowal A, Freed PW, Westcott JY, Henson PM. Macrophages that have ingested apoptotic cells in vitro inhibit proinflammatory cytokine production through autocrine/paracrine mechanisms involving TGF-beta, PGE2, and PAF. The Journal of clinical investigation. 1998; 101:890–898. [PubMed: 9466984]
31. Varia MA, Calkins-Adams DP, Rinker LH, Kennedy AS, Novotny DB, Fowler WC Jr, Raleigh JA. Pimonidazole: a novel hypoxia marker for complementary study of tumor hypoxia and cell proliferation in cervical carcinoma. Gynecol Oncol. 1998; 71:270–277. [PubMed: 9826471]
32. Berra E, Benizri E, Ginouves A, Volmat V, Roux D, Pouyssegur J. HIF prolyl-hydroxylase 2 is the key oxygen sensor setting low steady-state levels of HIF-1alpha in normoxia. Embo J. 2003; 22:4082–4090. [PubMed: 12912907]
33. Appelhoff RJ, Tian YM, Raval RR, Turley H, Harris AL, Pugh CW, Ratcliffe PJ, Gleadle JM. Differential function of the prolyl hydroxylases PHD1, PHD2, and PHD3 in the regulation of hypoxia-inducible factor. The Journal of biological chemistry. 2004; 279:38458–38465. [PubMed: 15247232]

Author Manuscript Author Manuscript Author Manuscript Author Manuscript

34. Elomaa O, Kangas M, Sahlberg C, Tuukkanen J, Sormunen R, Liakka A, Thesleff I, Kraal G, Tryggvason K. Cloning of a novel bacteria-binding receptor structurally related to scavenger receptors and expressed in a subset of macrophages. Cell. 1995; 80:603–609. [PubMed: 7867067]
35. Xu J, Wang B, Xu Y, Sun L, Tian W, Shukla D, Barod R, Grillari J, Grillari-Voglauer R, Maxwell PH, Esteban MA. Epigenetic regulation of HIF-1alpha in renal cancer cells involves HIF-1alpha/2alpha binding to a reverse hypoxia-response element. Oncogene. 2012; 31:1065–1072. [PubMed: 21841824]
36. Pawlus MR, Wang L, Ware K, Hu CJ. Upstream stimulatory factor 2 and hypoxia-inducible factor 2alpha (HIF2alpha) cooperatively activate HIF2 target genes during hypoxia. Mol Cell Biol. 2012; 32:4595–4610. [PubMed: 22966206]
37. Harvey CJ, Thimmulappa RK, Sethi S, Kong X, Yarmus L, Brown RH, Feller-Kopman D, Wise R, Biswal S. Targeting Nrf2 signaling improves bacterial clearance by alveolar macrophages in patients with COPD and in a mouse model. Sci Transl Med. 2011; 3:3002042.
38. Zhang J, Ohta T, Maruyama A, Hosoya T, Nishikawa K, Maher JM, Shibahara S, Itoh K, Yamamoto M. BRG1 interacts with Nrf2 to selectively mediate HO-1 induction in response to oxidative stress. Mol Cell Biol. 2006; 26:7942–7952. [PubMed: 16923960]
39. Morimitsu Y, Nakagawa Y, Hayashi K, Fujii H, Kumagai T, Nakamura Y, Osawa T, Horio F, Itoh K, Iida K, Yamamoto M, Uchida K. A sulforaphane analogue that potently activates the Nrf2-dependent detoxification pathway. The Journal of biological chemistry. 2002; 277:3456–3463. [PubMed: 11706044]
40. Oktay Y, Dioum E, Matsuzaki S, Ding K, Yan LJ, Haller RG, Szweda LI, Garcia JA. Hypoxia-inducible factor 2alpha regulates expression of the mitochondrial aconitase chaperone protein frataxin. The Journal of biological chemistry. 2007; 282:11750–11756. [PubMed: 17322295]
41. Chandel NS, McClintock DS, Feliciano CE, Wood TM, Melendez JA, Rodriguez AM, Schumacker PT. Reactive oxygen species generated at mitochondrial complex III stabilize hypoxia-inducible factor-1alpha during hypoxia: a mechanism of O2 sensing. The Journal of biological chemistry. 2000; 275:25130–25138. [PubMed: 10833514]
42. Hamanaka RB, Glasauer A, Hoover P, Yang S, Blatt H, Mullen AR, Getsios S, Gottardi CJ, DeBerardinis RJ, Lavker RM, Chandel NS. Mitochondrial reactive oxygen species promote epidermal differentiation and hair follicle development. Science signaling. 2013; 6:ra8. [PubMed: 23386745]
43. Morelli AE, Larregina AT, Shufesky WJ, Zahorchak AF, Logar AJ, Papworth GD, Wang Z, Watkins SC, Falo LD, Thomson AW. Internalization of circulating apoptotic cells by splenic marginal zone dendritic cells: dependence on complement receptors and effect on cytokine production. Blood. 2003; 101:611–620. [PubMed: 12393562]
44. van der Laan LJ, Dopp EA, Haworth R, Pikkarainen T, Kangas M, Elomaa O, Dijkstra CD, Gordon S, Tryggvason K, Kraal G. Regulation and functional involvement of macrophage scavenger receptor MARCO in clearance of bacteria in vivo. J Immunol. 1999; 162:939–947. [PubMed: 9916718]
45. Arredouani MS, Palecanda A, Koziel H, Huang YC, Imrich A, Sulahian TH, Ning YY, Yang Z, Pikkarainen T, Sankala M, Vargas SO, Takeya M, Tryggvason K, Kobzik L. MARCO is the major binding receptor for unopsonized particles and bacteria on human alveolar macrophages. J Immunol. 2005; 175:6058–6064. [PubMed: 16237101]
46. Takeda N, O'Dea EL, Doedens A, Kim JW, Weidemann A, Stockmann C, Asagiri M, Simon MC, Hoffmann A, Johnson RS. Differential activation and antagonistic function of HIF-{alpha} isoforms in macrophages are essential for NO homeostasis. Genes Dev. 2010; 24:491–501. [PubMed: 20194441]
47. Jozefowski S, Arredouani M, Sulahian T, Kobzik L. Disparate regulation and function of the class A scavenger receptors SR-AI/II and MARCO. J Immunol. 2005; 175:8032–8041. [PubMed: 16339540]
48. Varin A, Mukhopadhyay S, Herbein G, Gordon S. Alternative activation of macrophages by IL-4 impairs phagocytosis of pathogens but potentiates microbial-induced signalling and cytokine secretion. Blood. 2010; 115:353–362. [PubMed: 19880493]
49. Sena LA, Chandel NS. Physiological roles of mitochondrial reactive oxygen species. Mol Cell. 2012; 48:158–167. [PubMed: 23102266]

Author Manuscript Author Manuscript Author Manuscript Author Manuscript

50. Ivan M, Kondo K, Yang H, Kim W, Valiando J, Ohh M, Salic A, Asara JM, Lane WS, Kaelin WG Jr. HIFalpha targeted for VHL-mediated destruction by proline hydroxylation: implications for O2 sensing. Science. 2001; 292:464–468. [PubMed: 11292862]
51. West AP I, Brodsky E, Rahner C, Woo DK, Erdjument-Bromage H, Tempst P, Walsh MC, Choi Y, Shadel GS, Ghosh S. TLR signalling augments macrophage bactericidal activity through mitochondrial ROS. Nature. 2011; 472:476–480. [PubMed: 21525932]
52. van der Laan LJ, Dopp EA, Haworth R, Pikkarainen T, Kangas M, Elomaa O, Dijkstra CD, Gordon S, Tryggvason K, Kraal G. Regulation and functional involvement of macrophage scavenger receptor MARCO in clearance of bacteria in vivo. Journal of Immunology. 1999; 162:939–947.
53. Nishi C, Toda S, Segawa K, Nagata S. Tim4- and MerTK-mediated engulfment of apoptotic cells by mouse resident peritoneal macrophages. Mol Cell Biol. 2014; 34:1512–1520. [PubMed: 24515440]
54. Kuschel A, Simon P, Tug S. Functional regulation of HIF-1alpha under normoxia--is there more than post-translational regulation? J Cell Physiol. 2012; 227:514–524. [PubMed: 21503885]
55. Ranasinghe WK, Baldwin GS, Shulkes A, Bolton D, Patel O. Normoxic regulation of HIF-1alpha in prostate cancer. Nat Rev Urol. 2014 Jul.11(7):419. Epub 2014 Jul 1. doi: 10.1038/nrurol.2013.110-c2
56. Stroka DM, Burkhardt T, Desbaillets I, Wenger RH, Neil DA, Bauer C, Gassmann M, Candinas D. HIF-1 is expressed in normoxic tissue and displays an organ-specific regulation under systemic hypoxia. Faseb J. 2001; 15:2445–2453. [PubMed: 11689469]
57. Piccoli C, D'Aprile A, Ripoli M, Scrima R, Boffoli D, Tabilio A, Capitanio N. The hypoxia-inducible factor is stabilized in circulating hematopoietic stem cells under normoxic conditions. FEBS letters. 2007; 581:3111–3119. [PubMed: 17568584]
58. Maxwell PH, Wiesener MS, Chang GW, Clifford SC, Vaux EC, Cockman ME, Wykoff CC, Pugh CW, Maher ER, Ratcliffe PJ. The tumour suppressor protein VHL targets hypoxia-inducible factors for oxygen-dependent proteolysis. Nature. 1999; 399:271–275. [PubMed: 10353251]
59. Weidemann A, Johnson RS. Biology of HIF-1alpha. Cell Death Differ. 2008; 15:621–627. [PubMed: 18259201]
60. Herr B, Zhou J, Werno C, Menrad H, Namgaladze D, Weigert A, Dehne N, Brune B. The supernatant of apoptotic cells causes transcriptional activation of hypoxia-inducible factor-1alpha in macrophages via sphingosine-1-phosphate and transforming growth factor-beta. Blood. 2009; 114:2140–2148. [PubMed: 19549990]
61. Fang HY, Hughes R, Murdoch C, Coffelt SB, Biswas SK, Harris AL, Johnson RS, Imityaz HZ, Simon MC, Fredlund E, Greten FR, Rius J, Lewis CE. Hypoxia-inducible factors 1 and 2 are important transcriptional effectors in primary macrophages experiencing hypoxia. Blood. 2009; 114:844–859. [PubMed: 19454749]
62. Bosco MC, Puppo M, Santangelo C, Anfosso L, Pfeffer U, Fardin P, Battaglia F, Varesio L. Hypoxia modifies the transcriptome of primary human monocytes: modulation of novel immune-related genes and identification of CC-chemokine ligand 20 as a new hypoxia-inducible gene. J Immunol. 2006; 177:1941–1955. [PubMed: 16849508]
63. Hu CJ, Wang LY, Chodosh LA, Keith B, Simon MC. Differential roles of hypoxia-inducible factor 1alpha (HIF-1alpha) and HIF-2alpha in hypoxic gene regulation. Mol Cell Biol. 2003; 23:9361–9374. [PubMed: 14645546]
64. Anand RJ, Gribar SC, Li J, Kohler JW, Branca MF, Dubowski T, Sodhi CP, Hackam DJ. Hypoxia causes an increase in phagocytosis by macrophages in a HIF-1alpha-dependent manner. J Leukoc Biol. 2007; 82:1257–1265. [PubMed: 17675562]
65. Werno C, Menrad H, Weigert A, Dehne N, Goerdt S, Schledzewski K, Kzhyshkowska J, Brune B. Knockout of HIF-1alpha in tumor-associated macrophages enhances M2 polarization and attenuates their pro-angiogenic responses. Carcinogenesis. 2010; 31:1863–1872. [PubMed: 20427344]
66. Fukuzumi M, Shinomiya H, Shimizu Y, Ohishi K, Utsumi S. Endotoxin-induced enhancement of glucose influx into murine peritoneal macrophages via GLUT1. Infect Immun. 1996; 64:108–112. [PubMed: 8557327]

Author Manuscript Author Manuscript Author Manuscript Author Manuscript

67. Nagy C, Haschemi A. Time and Demand are Two Critical Dimensions of Immunometabolism: The Process of Macrophage Activation and the Pentose Phosphate Pathway. Frontiers in immunology. 2015; 6:164. [PubMed: 25904920]
68. Talks KL, Turley H, Gatter KC, Maxwell PH, Pugh CW, Ratcliffe PJ, Harris AL. The expression and distribution of the hypoxia-inducible factors HIF-1alpha and HIF-2alpha in normal human tissues, cancers, and tumor-associated macrophages. The American journal of pathology. 2000; 157:411–421. [PubMed: 10934146]
69. Eubank TD, Roda JM, Liu H, O'Neil T, Marsh CB. Opposing roles for HIF-1alpha and HIF-2alpha in the regulation of angiogenesis by mononuclear phagocytes. Blood. 2011; 117:323–332. [PubMed: 20952691]
70. Choe SS, Shin KC, Ka S, Lee YK, Chun JS, Kim JB. Macrophage HIF-2alpha ameliorates adipose tissue inflammation and insulin resistance in obesity. Diabetes. 2014; 63:3359–3371. [PubMed: 24947359]
71. Crucet M, Wust SJ, Spielmann P, Luscher TF, Wenger RH, Matter CM. Hypoxia enhances lipid uptake in macrophages: role of the scavenger receptors Lox1, SRA, and CD36. Atherosclerosis. 2013; 229:110–117. [PubMed: 23706521]
72. Shirato K, Kizaki T, Sakurai T, Ogasawara JE, Ishibashi Y, Iijima T, Okada C, Noguchi I, Imaizumi K, Taniguchi N, Ohno H. Hypoxia-inducible factor-1alpha suppresses the expression of macrophage scavenger receptor 1. Pflugers Arch. 2009; 459:93–103. [PubMed: 19641936]
73. Marsch E, Theelen TL, Demandt JA, Jeurissen M, van Gink M, Verjans R, Janssen A, Cleutjens JP, Meex SJ, Donners MM, Haenen GR, Schalkwijk CG, Dubois LJ, Lambin P, Mallat Z, Gijbels MJ, Heemskerk JW, Fisher EA, Biessen EA, Janssen BJ, Daemen MJ, Sluimer JC. Reversal of hypoxia in murine atherosclerosis prevents necrotic core expansion by enhancing efferocytosis. Arterioscler Thromb Vasc Biol. 2014; 34:2545–2553. [PubMed: 25256233]
74. Toth B, Garabuczi E, Sarang Z, Vereb G, Vamosi G, Aeschlimann D, Blasko B, Becsi B, Erdodi F, Lacy-Hulbert A, Zhang A, Falasca L, Birge RB, Balajthy Z, Melino G, Fesus L, Szondy Z. Transglutaminase 2 is needed for the formation of an efficient phagocyte portal in macrophages engulfing apoptotic cells. J Immunol. 2009; 182:2084–2092. [PubMed: 19201861]
75. Filiano AJ, Bailey CD, Tucholski J, Gundemir S, Johnson GV. Transglutaminase 2 protects against ischemic insult, interacts with HIF1beta, and attenuates HIF1 signaling. Faseb J. 2008; 22:2662–2675. [PubMed: 18375543]
76. Louis NA, Hamilton KE, Kong T, Colgan SP. HIF-dependent induction of apical CD55 coordinates epithelial clearance of neutrophils. Faseb J. 2005; 19:950–959. [PubMed: 15923405]
77. Hatsuzawa K, Hashimoto H, Arai S, Tamura T, Higa-Nishiyama A, Wada I. Sec22b is a negative regulator of phagocytosis in macrophages. Mol Biol Cell. 2009; 20:4435–4443. [PubMed: 19710423]
78. Brunelle JK, Bell EL, Quesada NM, Vercauteren K, Tiranti V, Zeviani M, Scarpulla RC, Chandel NS. Oxygen sensing requires mitochondrial ROS but not oxidative phosphorylation. Cell Metab. 2005; 1:409–414. [PubMed: 16054090]
79. Scortegagna M, Ding K, Oktay Y, Gaur A, Thurmond F, Yan LJ, Marck BT, Matsumoto AM, Shelton JM, Richardson JA, Bennett MJ, Garcia JA. Multiple organ pathology, metabolic abnormalities and impaired homeostasis of reactive oxygen species in Epas1−/− mice. Nat Genet. 2003; 35:331–340. [PubMed: 14608355]
80. Kumar GK, Peng YJ, Nanduri J, Prabhakar NR. Carotid Body Chemoreflex Mediates Intermittent Hypoxia-Induced Oxidative Stress in the Adrenal Medulla. Adv Exp Med Biol. 2015; 860:195–199. [PubMed: 26303481]
81. Kim W, Kim HU, Lee HN, Kim SH, Kim C, Cha YN, Joe Y, Chung HT, Jang J, Kim K, Suh YG, Jin HO, Lee JK, Surh YJ. Taurine Chloramine Stimulates Efferocytosis Through Upregulation of Nrf2-Mediated Heme Oxygenase-1 Expression in Murine Macrophages: Possible Involvement of Carbon Monoxide. Antioxid Redox Signal. 2015; 23:163–177. [PubMed: 25816687]
82. Thompson AA, Elks PM, Marriott HM, Eamsamarng S, Higgins KR, Lewis A, Williams L, Parmar S, Shaw G, McGrath EE, Formenti F, Van Eeden FJ, Kinnula VL, Pugh CW, Sabroe I, Dockrell DH, Chilvers ER, Robbins PA, Percy MJ, Simon MC, Johnson RS, Renshaw SA, Whyte MK, Walmsley SR. Hypoxia-inducible factor 2alpha regulates key neutrophil functions in humans, mice, and zebrafish. Blood. 2014; 123:366–376. [PubMed: 24196071]

Author Manuscript Author Manuscript Author Manuscript Author Manuscript

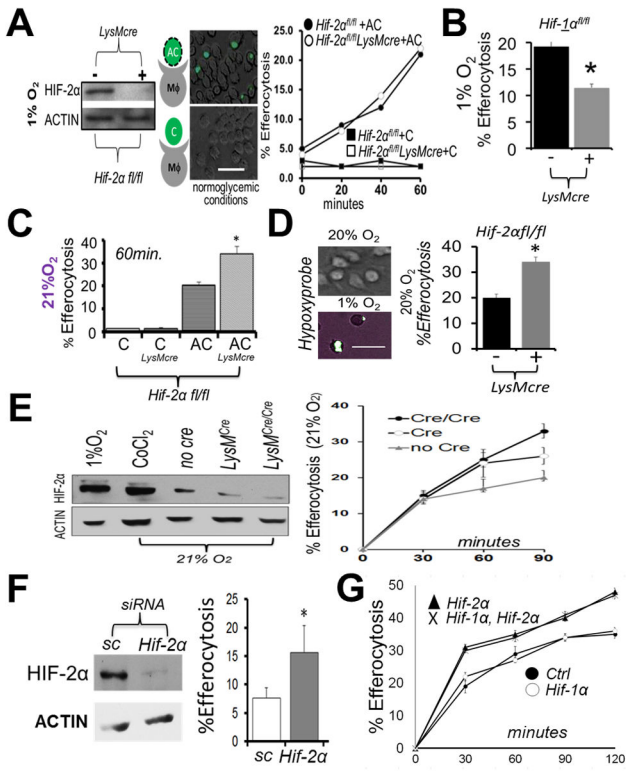

Figure 1. *Hif-2α* is not required for hypoxic efferocytosis, in contrast to under non-hypoxic conditions, where *Hif-2α* specifically acts as an efferocytic suppressor

(**A)** Immunoblot of *Hif-2α*$^{fl/fl}$ *LysMcre* bone marrow-derived macrophages (Mϕs) after culture at 1% oxygen. Mϕs were overlaid with fluorescent (calcein-AM) apoptotic *Jurkat* T-cells (“AC”) or fluorescent viable *Jurkat* T-cells (“C”) and efferocytosis quantified. Scale bar = 60 micrometers. (**B**) Efferocytosis carried out similar to as in (A) except during with *Hif-1α*$^{fl/fl}$ *vs. Hif-1α*$^{fl/fl}$ *LysMcre Mϕs*. (**C)** Efferocytosis similar to as in (A) except under normoxia. **(D)** Efferocytosis by *Hif-2α*$^{fl/fl}$ *vs Hif-2α*$^{fl/fl}$ *LysMcre* phagocytes cultured on gas permeable plates. Wild type cultures were grown on Lumox plates to optimize gas exchange at indicated oxygen tensions and stained with hypoxyprobe (green) as an indicator of hypoxia. Efferocytosis of fluorescent apoptotic Jurkat cells by *Hif-2α*$^{fl/fl}$ *vs. Hif-2α*$^{fl/fl}$ *LysMcre* phagocytes after quantification by microscopy. **(E)** Immunoblots of HIF-2α levels as a function of efferocytosis efficiency. (**F)** Immunoblot of normoxic Mϕ HIF-2α after *Hif-2α* siRNA in mature Mϕs and % Efferocytosis at 30min. *Sc* = scrambled siRNA. (**G**) Normoxic efferocytosis kinetics of *Hif-2α*$^{fl/fl}$ *LysMcre vs. Hif-1α*$^{fl/fl}$ *Hif-2α*$^{fl/fl}$ *LysMcre vs. Hif-1α*$^{fl/fl}$ *LysMcre* vs. control (*Hif- 1α*$^{fl/fl}$ *Hif-2α*$^{fl/fl}$). * indicates < 0.05 relative to control.

Author Manuscript Author Manuscript Author Manuscript Author Manuscript

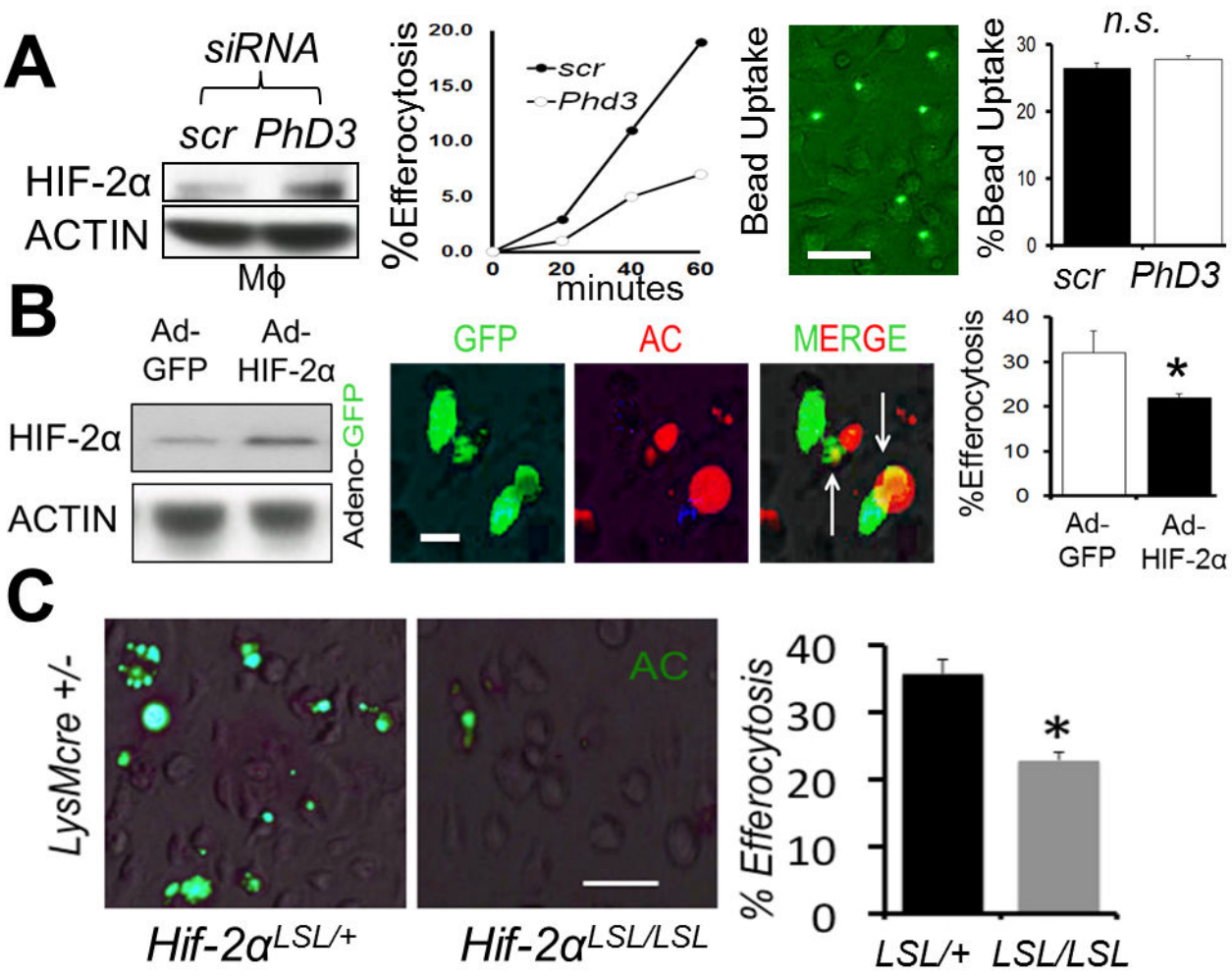

Figure 2. Strategies that induce HIF-2α are sufficient to suppress efferocytosis

(A) Bone marrow-derived Mϕs were treated with *scrambled (scr) vs. Phd3 siRNA* and HIF-2α levels revealed by immunoblot, as a function of efferocytosis and engulfment of control latex beads. (**B**) Adeno-HIF-2α-GFP (green) was transduced into Mϕs and immunoblots and efferocytosis of red apoptotic cells (ACs) quantified. (**C**) Non-stained primary *Hif-2α* $^{LSL/+}$ *LysMcre* vs. *Hif-2α* $^{LSL/LSL}$ *LysMcre* Mϕs were challenged with ACs and efferocytosis imaged and quantified. Scale bar = 60 micrometers. * indicates < 0.05 relative to control.

Author Manuscript Author Manuscript Author Manuscript Author Manuscript

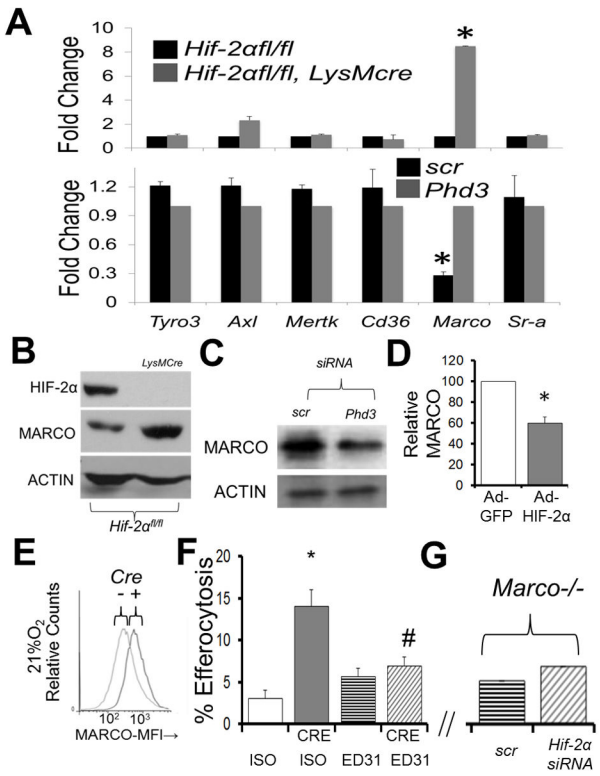

Figure 3. *Hif-2α* deficiency enhances MARCO expression in primary mouse Mϕs, which is required for enhanced efferocytosis

(**A**) qPCR data of indicated receptors from *Hif-2α*$^{fl/fl}$ *LysMcre* (TOP) vs after *Phd3 siRNA* from Mϕs under normoxic conditions. **(B)** Immunoblot of MARCO in *Hif-2α*$^{fl/fl}$ *vs. Hif-2α*$^{fl/fl}$ *LysMcre Mϕs* under normoxia. **(C)** Immunoblot of MARCO after *PhD3 siRNA* in Mϕs under normoxia. (**D**) Densitometry of MARCO protein after adenoviral *Hif-2α* expression under normoxia. (**E**) Cell surface flow cytometry of MARCO in *Hif-2α*$^{fl/fl}$ *vs. Hif-2α*$^{fl/fl}$ *LysMcre* Mϕs. **(F)** *Hif-2α*$^{fl/fl}$ versus *Hif2α*$^{fl/fl}$ *LysMcre* (CRE) primary Mϕs were treated with 10μg/mL MARCO blocking antibody (clone ED31, azide-free) or IgG1 isotype (ISO) control prior to co-culture with fluorescently-labelled apoptotic cells and efferocytosis enumerated. * indicates $p < 0.05$ vs. ISO control and # indicates $p < 0.04$ vs. CRE/ISO control. **(G)** *Marco−/−* Mϕs were treated with *Hif-2α* siRNA and challenged with apoptotic cells (Bar graph axis same as in (F).

Author Manuscript Author Manuscript Author Manuscript Author Manuscript

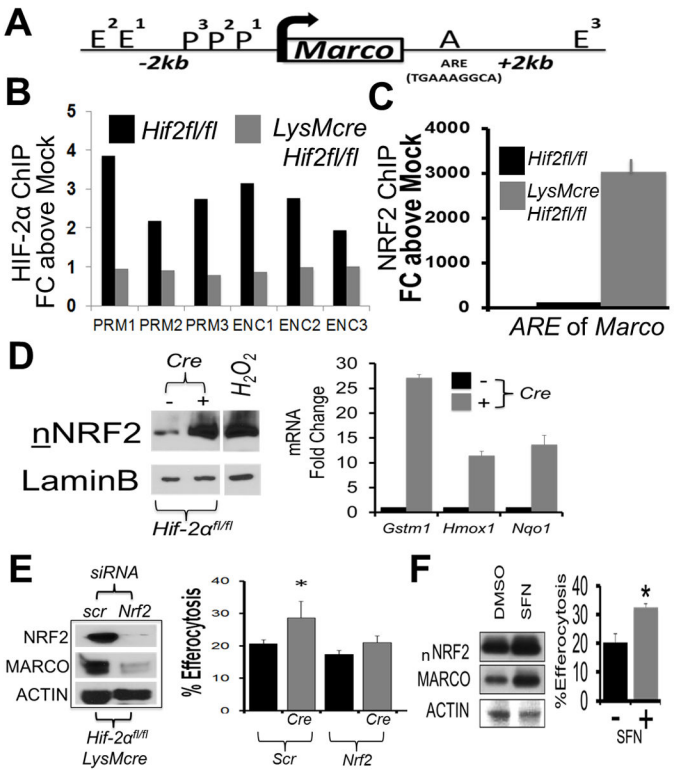

Figure 4. Minimal HIF-2α association with *Marco*, in contrast to NRF2, which is required for enhanced efferocytosis

(A) Schematic of *Marco* gene regulator regions, including Enhancer (E), Promoter (P), and ARE element. (**B**) Chromatin precipitation for HIF-2α on *3 P (PRM1-3)* and *3 E (ENC1-3)* regions each. **(C)** Chromatin precipitation for NRF2 on *Marco*. (**D**) Nuclear translocation of NRF2 in control vs *Hif-2α fl/fl LysMcre* Mϕs and induction of indicated NRF2 target genes. (**E**) *Nrf2 siRNA* tests (vs scrambled/scr) reduces MARCO in *Hif-2α fl/fl LysMcre* Mϕs. Efferocytosis efficiency in control *Hif-2α fl/fl* vs. *Hif-2α fl/fl LysMcre* Mϕs treated with indicated siRNA (Scr vs Nrf2). * indicates < 0.05 relative to control. **(F)** NRF2 agonist induces MARCO and enhances efferocytosis. WT bone marrow derived macrophages were treated with 20uM Sulforaphane, NRF2 agonist, for 24hrs, prior to blotting (nNRF2 = nuclear NRF2) and efferocytosis.

Author Manuscript Author Manuscript Author Manuscript Author Manuscript

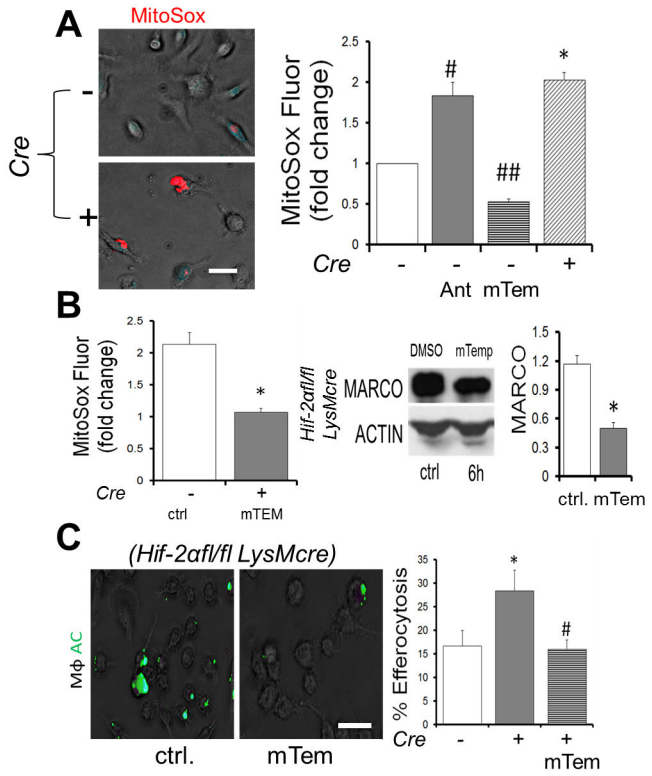

Figure 5. Elevated mROS increases MARCO & efferocytosis in the absence of *Hif-2α*

(**A**) Elevated mROS in *Hif-2α-deficient* Mϕs was measured vs. control with MitoSox. Antimycin A, an electron transport chain-inhibitor and positive control for mROS formation. mTempo was used to inhibit mROS. # and ## and * indicate $p < 0.05$ versus control. (**B**) mTEMPO reduces MitoSox mROS in *Hif-2α* deficient Mϕs and also suppresses MARCO. (**C**) Mito-Tempo reduces enhanced efferocytosis. Scale bar indicates 30 micrometers. * indicates $p < 0.05$ versus WT control. # indicates $p < 0.05$ versus knockout control.

Author Manuscript Author Manuscript Author Manuscript Author Manuscript

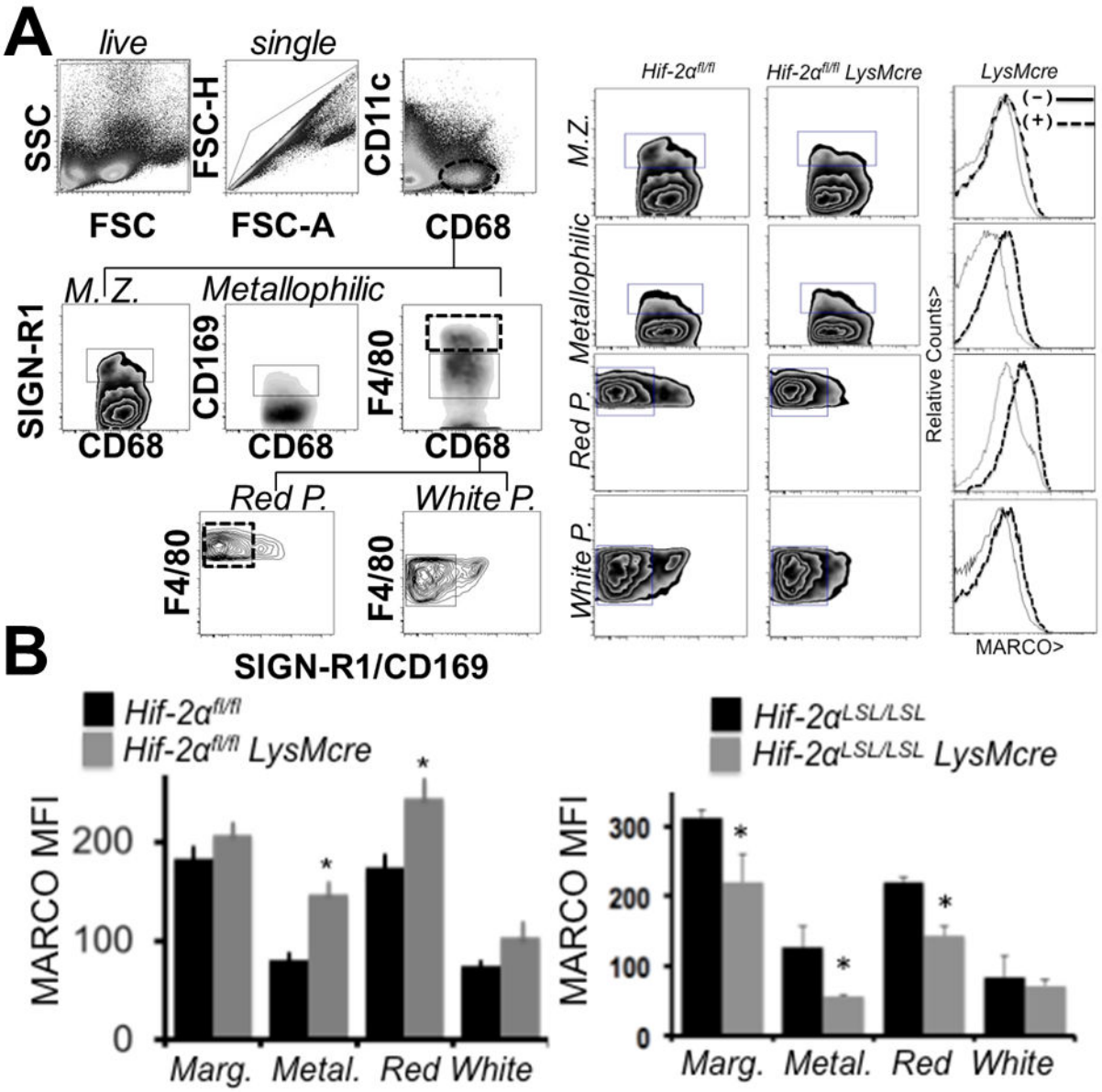

Figure 6. *Hif-2α*-MARCO axis is revealed in vivo

(**A**) Evidence for elevated MARCO protein on splenic macrophages from *Hif-2α*$^{fl/fl}$ *vs Hif-2α*$^{fl/fl}$ *LysMcre.* To the left is the gating strategy for splenic macrophage subsets. To the right are the analyses of the individual populations. (**B**) Quantification of elevations in MARCO expression (mean fluorescent intensity) in *Hif-2α*$^{fl/fl}$ *vs Hif-2α*$^{fl/fl}$ *LysMcre* mice and *Hif-2α* $^{LSL/LSL}$ mice vs. *Hif-2α* $^{LSL/LSL}$ *LysMcre mice.*

Author Manuscript Author Manuscript Author Manuscript Author Manuscript

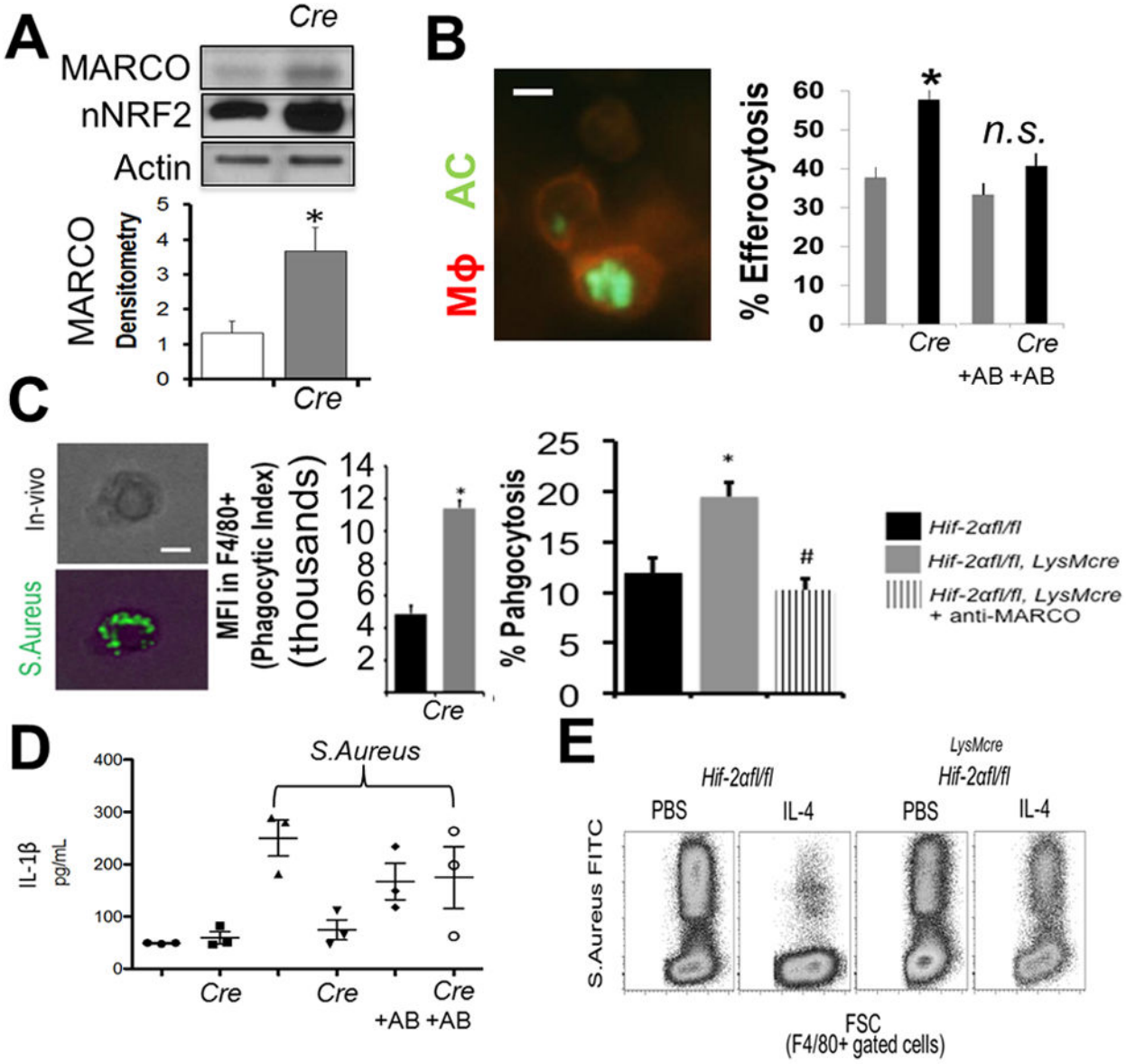

Figure 7. *Hif-2α-Marco* axis is functional *in vivo*

(**A**) Evidence for elevated MARCO protein and nuclear NRF2 in resident peritoneal Mϕs from *Hif-2α*$^{fl/fl}$ *vs. Hif-2α*$^{fl/fl}$ *LysMcre* mice after immunoblotting. (**B**) Peritoneal resident Mϕ efferocytosis after intraperitoneal injection of fluorescent apoptotic thymocytes (AC) into *Hif-2α*$^{fl/fl}$ *vs. Hif-2α*$^{fl/fl}$ *LysMcre* mice +/− AB (MARCO blocking antibody). **(C)** Acute phagocytosis of *S. Aureus* is enhanced in the absence of *Hif-2α* through MARCO. Heat-killed FITC-labeled *S. Aureus* were injected into the peritoneum of *Hif-2α-deficient* mice and % phagocytosis by resident F4/80+ phagocytes enumerated. Anti-MARCO antibody was added prior to bacterial injection. (**D**) Plasma cytokine levels were examined in *Hif-2α*$^{fl/fl}$ vs *Hif-2α*$^{fl/fl}$ *LysMcre* mice after injection of *S. Aureus* vs. PBS vehicle and +/−

MARCO blocking antibody vs. isotype control. (**E**) IL-4 suppression of F4/80-gated macrophage phagocytosis under saturating MOI requires *Hif-2a*.

Author Manuscript Author Manuscript Author Manuscript Author Manuscript